



Research Paper

The uremic toxin hippurate promotes endothelial dysfunction via the activation of Drp1-mediated mitochondrial fission

Mengjie Huang, Ribao Wei*, Yang Wang, Tingyu Su, Ping Li, Xiangmei Chen

Department of Nephrology, Chinese PLA General Hospital, Chinese PLA Institute of Nephrology, State Key Laboratory of Kidney Diseases, National Clinical Research Center for Kidney Diseases, Beijing Key Laboratory of Kidney Disease, Beijing 100853, People's Republic of China



ARTICLE INFO

Keywords:

Hippurate
Chronic kidney disease
Endothelial dysfunction
Mitochondrial fission
Oxidative stress

ABSTRACT

The accumulation of uremic toxins in chronic kidney disease (CKD) induces inflammation, oxidative stress and endothelial dysfunction, which is a key step in atherosclerosis. Accumulating evidence indicates increased mitochondrial fission is a contributing mechanism for impaired endothelial function. Hippurate, a uremic toxin, has been reported to be involved in cardiovascular diseases. Here, we assessed the endothelial toxicity of hippurate and the contribution of altered mitochondrial dynamics to hippurate-induced endothelial dysfunction.

Treatment of human aortic endothelial cells with hippurate reduced the expression of endothelial nitric oxide synthase (eNOS) and increased the expression of intercellular cell adhesion molecule-1 (ICAM-1) and von Willebrand factor (vWF). The mechanisms of hippurate-induced endothelial dysfunction in vitro depended on the activation of Dynamin-related protein 1 (Drp1)-mediated mitochondrial fission and overproduction of mitochondrial reactive oxygen species (mitoROS). In a rat model in which CKD was induced by 5/6 nephrectomy (CKD rat), we observed increased oxidative stress, impaired endothelium-dependent vasodilation, and elevated soluble biomarkers of endothelial dysfunction (ICAM-1 and vWF). Similarly, endothelial dysfunction was identified in healthy rats treated with disease-relevant concentrations of hippurate. In aortas of CKD rats and hippurate-treated rats, we observed an increase in Drp1 protein levels and mitochondrial fission. Inhibition of Drp1 improved endothelial function in both rat models.

These results indicate that hippurate, by itself, can cause endothelial dysfunction. Increased mitochondrial fission plays an active role in hippurate-induced endothelial dysfunction via an increase in mitoROS.

1. Introduction

Cardiovascular disease (CVD) is a major factor affecting the prognosis of patients with chronic kidney disease (CKD), among whom the morbidity and mortality are respectively 10- to 20-fold higher than those in age- and sex-matched healthy people [1,2]. Endothelial dysfunction, including inappropriate regulation of vascular tone, activated inflammatory response and impaired antithrombotic property, is a key step in the development of atherosclerotic CVD [3,4]. Accumulating evidence indicates that endothelial dysfunction occurs in patients with CKD [5,6]. Although CKD patients have increased levels of traditional cardiovascular risk factors, i.e., hypertension, diabetes and hyperlipidemia [7], these factors cannot fully explain the high risk of CVD in patients with CKD. Accumulating evidence shows that the

accumulation of uremic toxins also play a vital role in CKD-associated endothelial dysfunction [8].

Protein-bound toxins cause damage to multiple organs due to poor clearance by dialysis [9,10]. Hippurate, an example of such a toxin, mainly comes from plant food and exists in the human body at a level of < 5 mg/l. In patients with CKD, hippurate concentration dramatically increases and can become as high as 471 mg/l (2.6 mmol/l) [10]. Recent studies have suggested that hippurate can increase reactive oxygen species (ROS) production in endothelial cells [9], and may be involved in endothelial dysfunction [11]. Besides, with the increase in serum hippurate level, the tendency of cardiovascular mortality and all-cause mortality of patients with end-stage renal disease (ESRD) increases [12,13]. All the evidences indicate that hippurate may play a certain role in promoting endothelial dysfunction and CVD in CKD

Abbreviations: Ach, Acetylcholine; CCK8, Cell Counting Kit-8; CVD, cardiovascular disease; CKD, chronic kidney disease; DHE, dihydroethidium; Drp1, Dynamin-related protein 1; ESRD, end-stage renal disease; eNOS, endothelial nitric oxide synthase; Fis1, fission 1; HAECs, human aortic endothelial cells; ICAM-1, intercellular cell adhesion molecule-1; Mdivi-1, mitochondrial division inhibitor 1; mitoROS, mitochondrial ROS; Mff, mitochondrial fission factor; PE, phenylephrine hydrochloride; qRT-PCR, quantitative reverse transcription polymerase chain reaction; ROS, reactive oxygen species; SNP, sodium nitroprusside; siRNA, small interfering RNA; vWF, von Willebrand factor

* Corresponding author.

E-mail address: wrbj2006@126.com (R. Wei).

<https://doi.org/10.1016/j.redox.2018.03.010>

Received 22 February 2018; Received in revised form 14 March 2018; Accepted 15 March 2018

Available online 16 March 2018

2213-2317/ © 2018 The Authors. Published by Elsevier B.V. This is an open access article under the CC BY-NC-ND license (<http://creativecommons.org/licenses/by-nc-nd/4.0/>).

patients. However, the underlying mechanisms remain unclear.

Mitochondria are major sites for ROS production. In recent years, the dynamics of mitochondria, especially mitochondrial fusion and fission, has aroused widespread interest. Normally, mitochondrial fusion and fission are in dynamic equilibrium. The intact mitochondrial membrane structure helps to prevent excessive ROS production. When mitochondrial fission becomes dominant, mitochondrial fragmentation and ROS production increase. Dynamin-related protein 1 (Drp1) is the major regulator of mitochondrial fission. Increased Drp1 expression induces mitochondrial fission. Existing studies have demonstrated that Drp1-mediated mitochondrial fission can induce oxidative damage and promote endothelial dysfunction under conditions of high glucose or hypoxia/reoxygenation injury [14–16].

In the present study, we examined (1) endothelial toxicity due to hippurate in vitro and in vivo, (2) the role of Drp1, and (3) the relationship between Drp1-mediated mitochondrial fission and hippurate-induced endothelial dysfunction.

2. Materials and methods

2.1. Reagents

Hippurate and mitochondrial division inhibitor 1 (mdivi-1) were purchased from Sigma-Aldrich (USA). These agents were dissolved in dimethyl sulfoxide (DMSO) as a stock solution and the final working concentration of DMSO was < 0.1% (v/v). Acetylcholine (ACh), sodium nitroprusside (SNP) and phenylephrine hydrochloride (PE) were purchased from Sigma-Aldrich for assessment of relaxation in aortic rings. Primary antibodies information (name, company, catalogue number, molecular weight) was shown in [Supplemental Table 1](#).

2.2. Cell culture

Human aortic endothelial cells (HAECs) were purchased from ScienCell Research Laboratories and cultured with the endothelial cell medium supplemented with fetal bovine serum (5%v/v), penicillin (10,000 U/mL), streptomycin (10,000 µg/mL), and endothelial cell growth supplement at 37 °C in a humidified incubator under 5% CO₂ atmosphere. Only three to six passages of HAECs were used in these experiments.

2.3. RNA interference

For small interfering RNA (siRNA) treatment, we grew HAECs to approximately 50% confluence, transfected them using Lipofectamine RNAiMax (Invitrogen, USA) and validated the efficiency of transfection with Drp1-specific siRNA or a negative control siRNA (GenePharma, China). After 6 h, normal culture medium was added to the cells. Efficiency of knockdown was confirmed using quantitative reverse transcription polymerase chain reaction (qRT-PCR).

2.4. Animal models

Male Wistar rats were obtained from Beijing Vital River Laboratory Animal Technology Co. Ltd., China. The rats were housed in temperature-controlled cages under a 12-h light/12-h dark cycle with free access to food and water. An experimental CKD model was established in 6-week-old rats by 5/6 nephrectomy with a 2-step surgical procedure as previously described [17]. Briefly, the upper and lower poles of the right kidney were resected. One week later, the left kidney was removed after ligation of the renal blood vessels and the ureter. For the sham operation, only the adipose capsule was isolated, and the kidney tissue was retained. For the CKD model, we studied the following four groups (n = 6–7/group): (1) Sham group, sham-operated rats treated daily with DMSO as vehicle by intraperitoneal (i.p.) injections; (2) Sham + mdivi-1 group, sham-operated rats treated with mdivi-1 by i.p.

injections at a dose of 1.2 mg/kg/d; (3) CKD group, 5/6 nephrectomy-treated rats treated daily with DMSO as vehicle by i.p. injections; and (4) CKD + mdivi-1 group, 5/6 nephrectomy-treated rats treated with mdivi-1 by i.p. injections at a dose of 1.2 mg/kg/d.

To investigate the effect of hippurate on endothelial dysfunction, we established a chronic hippurate model. Healthy 6-week-old rats were given daily i.p. injections of 50 mg/kg hippurate or hippurate-free DMSO (control group) for 6 weeks. For the hippurate model, we studied the following four groups (n = 6–7/group): (1) Control group, healthy rats treated daily with DMSO as vehicle by i.p. injections; (2) Control + mdivi-1 group, healthy rats treated with mdivi-1 by i.p. injections at a dose of 1.2 mg/kg/d; (3) Hippurate group, healthy rats treated daily with hippurate by i.p. injections; and (4) Hippurate + mdivi-1 group, healthy rats treated with a mixture of hippurate and mdivi-1.

The animal protocol was reviewed and approved by the Institutional Animal Care and Use Committee of the Chinese PLA General Hospital.

2.5. Laboratory measurements

At the end of the experiment, the rats were intraperitoneally anesthetized with 2% pentobarbitalum natricum (Solarbio, China), and blood was obtained from abdominal aorta and centrifuged for 15 min at 3000 rpm to separate the serum.

Serum hippurate was measured by liquid chromatography tandem mass spectrometry (LC/MS). Hippurate was separated by a Dionex Ultimate 3000 RSLCnano system (Thermo Fisher Scientific, USA) using a Hypersil Gold column (2.1 × 100 mm, inner diameter 1.9 µm, Thermo Fisher Scientific). The column temperature was set to 20 °C, and 1 µl of sample was injected to the LC system at a flow rate of 0.5 mL/min. The mobile phase was composed of (A) 10 mmol/l ammonium formate in water and (B) acetonitrile (A:B=1:9). The mass spectrometer was operating with positive ionization in the selected reaction monitoring (SRM) mode. Electrospray settings of the assay were a 4002 V spray voltage and a 300 °C capillary temperature. High purity argon was used as the collision gas. Sheath gas pressure was 40 Arb and aux gas pressure (nitrogen, purity ≥ 99.9%) was 10 Arb. Hippurate was monitored at *m/z* 179.9→105 and the internal standard amitriptyline hydrochloride at *m/z* 278.2→91.0.

2.6. Measurement of endothelial function

Rat aortas were quickly dissected out after anesthesia, placed in Krebs–Henseleit solution (in mmol/l: NaCl 115, CaCl₂ 2.5, KCl 4.6, KH₂PO₄ 1.2, MgSO₄·7H₂O 1.2, NaHCO₃ 25, glucose 11.1, with a pH of 7.4) at 4 °C, and fat and connective tissue were cleaned off. The isolated aortas were cut into 3–4 mm sections and passed through the lumen of the vascular segment by 2 parallel steel triangles – one was fixed to an organ bath and the other connected to a tension transducer (TSD125B; Biopac) linked to AcqKnowledge software (MP150; Biopac). Aortic rings were bathed in 15 mL of Krebs–Henseleit solution, gassed with 95% O₂ + 5% CO₂ at 37 °C and equilibrated for 60 min with 2.0 g of basal tension as previously described [18]. After equilibration, the rings were incubated with 60 mmol/l KCl to determine maximum contractility. After washing, followed by equilibration for another 30 min, we evoked contractile response by PE (1 µmol/l) to elicit reproducible responses. At the plateau of contraction, accumulative ACh (10⁻⁹–10⁻⁵ mol/l) or SNP (10⁻⁹–10⁻⁶ mol/l) was added into the organ bath to induce endothelium-dependent/independent relaxation.

2.7. Cell viability assay

Cell Counting Kit-8 (CCK8, Dojindo, Japan) was used to assess the effect of hippurate on cell viability. HAECs were seeded at the density of 4000 cells/well in a 96-well plate and allowed to attach overnight for 24 h, then the medium was changed to fresh medium containing different concentrations of hippurate (0, 1, 2, 4 mmol/l). After treatment

for 48 h, 10 μ l CCK-8 reagent was added to per well and reacted for 4 h. Absorbance was evaluated at 450 nm using a microplate spectrophotometer (iMark™, Bio-Rad, USA). The relative cell viability of normal control group was taken as 100% of viability.

Cell viability of each group = $[(As-Ab) / (Ac-Ab)] \times 100\%$

As: Experimental wells (culture medium containing cells, CCK8 and hippurate)

Ac: Control wells (culture medium containing cells, CCK8, without hippurate)

Ab: Blank wells (culture medium containing CCK8, without cells and hippurate)

2.8. Assessment of total intracellular ROS and mitochondrial ROS

The levels of mitochondrial ROS (mitoROS) in HAECs were detected using MitoSOX Red dye (Invitrogen, USA). After treatment, cells were incubated in Hank's balanced salt solution containing 5 μ mol/l MitoSOX Red at 37 °C for 10 min in the dark. After incubation, the cells were rinsed twice with PBS to remove the dye. To visualize total intracellular ROS production in the vascular endothelium, freshly isolated aortas were stained with dihydroethidium (DHE, 10 μ mol/l, Beyotime, China) in a light-protected humidified chamber at 37 °C for 30 min. The fluorescence of MitoSOX Red and DHE was detected by fluorescence microscopy. Quantification of fluorescence intensity was measured using ImageJ software.

2.9. Electron microscopy

After treatment, cells and tissues were immediately fixed with 2.5% glutaraldehyde at 4 °C, post-fixed in 1% osmium tetroxide, dehydrated in graded methanol, and then embedded in epoxy resin (EMBed-812; Electron Microscopy Sciences, USA). A JEO-1400 transmission electron microscope was used to observe mitochondrial pathological changes.

2.10. Mitochondrial morphology and mitochondrial membrane potential analysis

The change in mitochondrial morphology was detected using MitoTracker Green (Beyotime). After treatment, cells were washed with PBS and then incubated with 100 nmol/l MitoTracker Green for 20 min at 37 °C. The structure of the mitochondria was observed by confocal microscopy. The mitochondrial membrane potential was detected using a JC-1 Kit (Beyotime), and images were obtained by a confocal laser-scanning microscope. Quantification of fluorescence intensity was measured using ImageJ software.

2.11. Western blot analysis

Western blot assays were used to analyze the protein expression of Drp1, fission 1 (Fis1), mitochondrial fission factor (Mff), endothelial nitric oxide synthase (eNOS), intercellular cell adhesion molecule-1 (ICAM-1), and von Willebrand factor (vWF). Cells and aorta tissues were lysed in RIPA buffer containing the protease inhibitor phenylmethanesulfonyl fluoride (PMSF), and the protein concentration was determined using the bicinchoninic acid (BCA) method. Total protein (50–80 μ g) was separated by sodium dodecyl sulfate-polyacrylamide gel electrophoresis (SDS-PAGE) and then transferred onto a nitrocellulose filter membranes, followed by incubation with primary antibodies against Drp1 (1:200), Mff (1:200), Fis1 (1:200), eNOS (1:1000), ICAM-1 (1:200), and vWF (1:200) overnight at 4 °C. After washing with Tris-buffered saline and Tween 20, the membrane was incubated with secondary antibody at room temperature for 60 min. The results were analyzed using ImageJ software. β -Actin was used as an internal reference.

2.12. Real-time PCR quantitative analysis

RNA was extracted from HAECs using TRIzol. The concentration of RNA was assessed using a NanoDrop 2000c spectrophotometer. The reverse transcription system included 5 \times RT master Mix (2 μ l, TOYOBO, Japan), RNA template (1 μ g), and RNase-free water in a final volume of 10 μ l. The reaction conditions were as follows: 37 °C for 15 min, 50 °C for 5 min, and 98 °C for 5 min. Real-time PCR was performed using a SYBR probe (Applied Biosystems, USA). An ABI 7900HT (Applied Biosystems, USA) thermocycler was used for qPCR amplifications. Relative expression (fold change vs. control) was calculated with the $2^{-\Delta\Delta Ct}$ method using glyceraldehyde-3-phosphate dehydrogenase (GAPDH) mRNA as the reference. The primer sequences used are shown in [Supplemental Table 2](#).

2.13. Immunohistochemical and immunofluorescence staining

Immunohistochemical staining was performed on paraffin sections of thoracic aortas by the avidin-biotin complex method to detect the expression of Drp1, eNOS, ICAM-1, and vWF as previously described [19]. The sections were manually analyzed with an Olympus IX51 biomedical image analysis system. Immunofluorescence staining was performed on aortic roots. Aorta slices were incubated overnight with primary antibodies at 4 °C. After rewarming at 37 °C for 1 h, the appropriate secondary antibodies were used. The nuclei were stained with 4',6-diamidino-2-phenylindole. The grade of fluorescence intensity was measured using ImageJ software.

2.14. Statistical analysis

All data are expressed as the mean \pm SD. Multiple measures of the same index at different time points were analyzed using multivariate repeated measures analysis of variance (ANOVA), and comparisons between groups at the same time point were performed using ANOVA for a completely randomized design. Pairwise comparisons of the means between multiple samples were conducted using Dunnett's *t*-test and the Student-Newman-Keuls (SNK)-*q* test. Two independent samples with normal distribution and homogeneity of variance were analyzed using *t*-tests. Multiple independent random samples were analyzed using single-factor ANOVA. Two-tailed *P* values less than 0.05 were considered statistically significant. Statistical analyses were performed using SPSS 19.0.

3. Results

3.1. Hippurate promotes endothelial dysfunction in a time- and dose-dependent manner

Hippurate, a protein-bound toxin, interacts negatively with biologic functions. In this study, we set four levels of hippurate (0, 1, 2, 4 mmol/l) based on serum hippurate concentrations of ESRD patients (2.6 mmol/l) and used CCK8 assay to evaluate whether hippurate can affect cell viability. As shown in [Supplemental Fig. 1](#), hippurate had no impact on cell viability at the concentrations used. To test the pro-inflammatory and pro-atherogenic effects of hippurate on the endothelium, we treated HAECs with increasing concentrations of hippurate at different stimulation time. Remarkably, hippurate reduced the protein and mRNA levels of eNOS and increased ICAM-1 and vWF expression in a time- ([Fig. 1A-C](#)) and dose-dependent manner ([Fig. 1D-F](#)).

3.2. Hippurate induces the mitochondrial ROS production, which contributes to endothelial dysfunction

Since many studies have found that ROS derived from mitochondria plays an active role in endothelial dysfunction [20], we used MitoSOX Red to detect whether hippurate could induce mitoROS production in

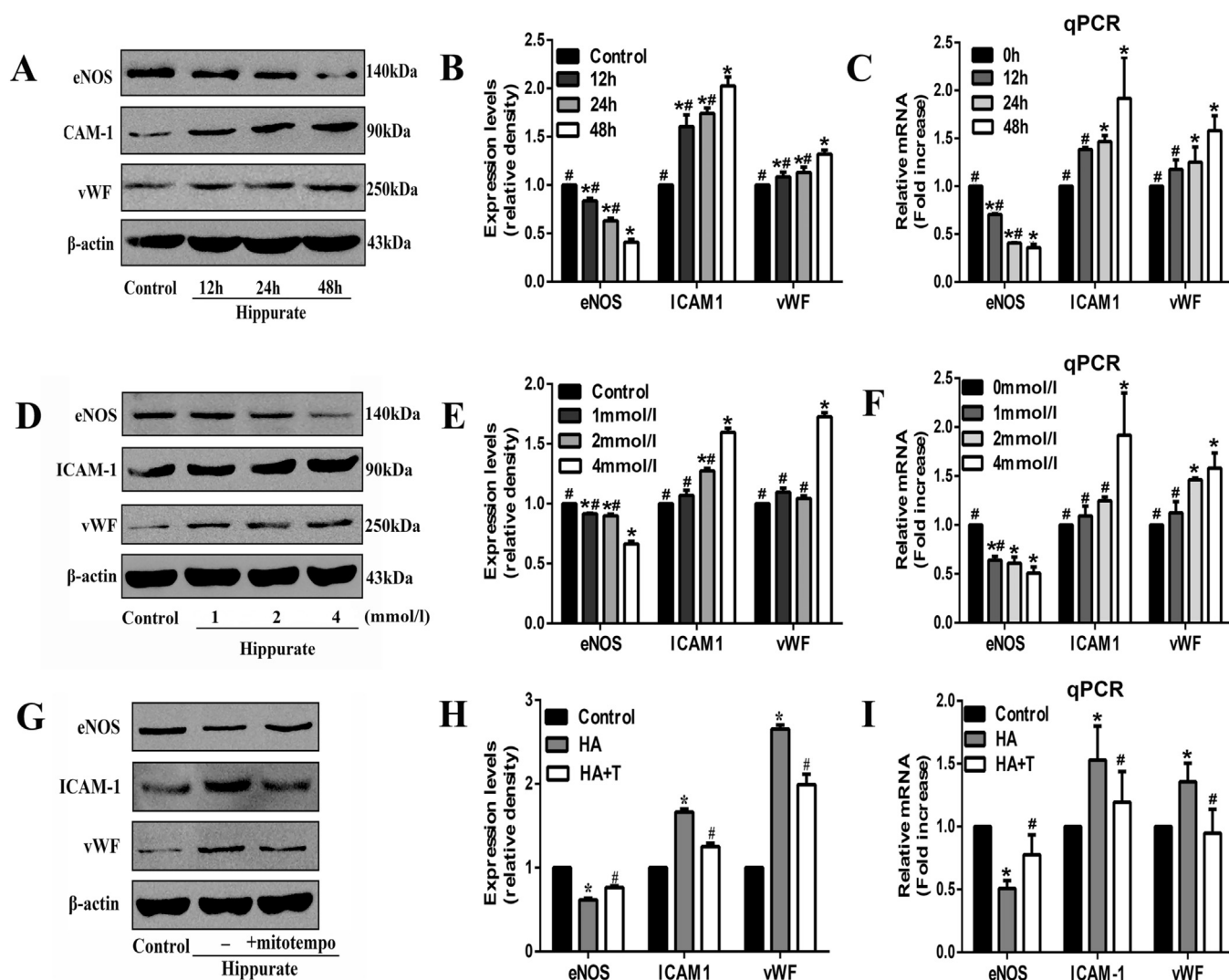


Fig. 1. Hippurate induces endothelial dysfunction via excessive mitochondrial ROS in vitro. Human aortic endothelial cells (HAECs) were treated with hippurate (1–4 mmol/l) for 12–48 h, in the presence or absence of mitochondrially targeted antioxidant MitoTEMPO (20 μ mol/l). A time-dependent (A–C) and dose-dependent (D–F) changes in the protein and mRNA levels of eNOS, ICAM-1 and vWF. The levels of protein and mRNA expression were normalized relative to non-treatment group (control). (G–I) MitoTEMPO increased eNOS and decreased ICAM-1, vWF at both protein and mRNA levels. * $P < 0.05$ vs. control, # $P < 0.05$ vs. 4 mmol/l 48 h hippurate.

endothelial cells. Of note, after stimulation with 4 mmol/l hippurate for 48 h, mitoROS levels were significantly elevated (Fig. 3A, B). To further demonstrate the role of mitoROS production in hippurate-induced endothelial dysfunction, we used the mitochondrially targeted antioxidant MitoTEMPO. When HAECs were pretreated with 20 μ mol/l MitoTEMPO for 2 h, mitoROS production was reduced to a relatively low level (Fig. 3A, B), and cell injury was mitigated, marked by an increased eNOS expression and decreased ICAM-1 and vWF expression (Fig. 1G–I). These results indicated that mitoROS contributes to hippurate-induced endothelial dysfunction.

3.3. Effect of hippurate on mitochondrial fission and dynamic proteins in human aortic endothelial cells

Previous studies have demonstrated that mitochondrial fission is an upstream causal factor for ROS overproduction [21]. To investigate whether hippurate induces mitoROS production by increasing mitochondrial fission, we first assessed mitochondrial morphology and the expression of mitochondrial fission-related proteins, including Drp1, Mff and Fis1, in HAECs exposed to hippurate. Under electron microscopy, the mitochondria in normal endothelial cells displayed a long rod-shaped morphology with integrated double membranes and tight

crisetae. In contrast, most mitochondria decreased in size and became punctate in hippurate-treated endothelial cells (Fig. 2A), indicating mitochondrial fragmentation. MitoTracker Green fluorescence indicated that normal mitochondria are elongated and tubular in shape forming highly interconnected networks, whereas hippurate induced numerous round mitochondrial fragments (Fig. 2B). In addition, western blot and qPCR results also showed that hippurate increased protein and mRNA levels of Drp1 without affecting the levels of Mff and Fis1 (Fig. 2C–E).

3.4. Drp1-mediated mitochondrial fragmentation triggers mitochondrial ROS production

We next used a Drp1 inhibitor to examine the contribution of Drp1 to mitochondrial fission and ROS production in hippurate-treated endothelial cells. As shown in Fig. 2F–H, Drp1-specific siRNA transfection significantly reduced the protein and mRNA levels of Drp1. The inhibition of Drp1 (with mdivi-1 and Drp1-specific siRNA) attenuated mitochondrial fragmentation in HAECs as demonstrated by immunofluorescence and electron microscopy (Fig. 2A, B). In addition, the inhibition of mitochondrial fragmentation by the Drp1 inhibitor normalized mitoROS levels (Fig. 3A, B). Moreover, we investigated the

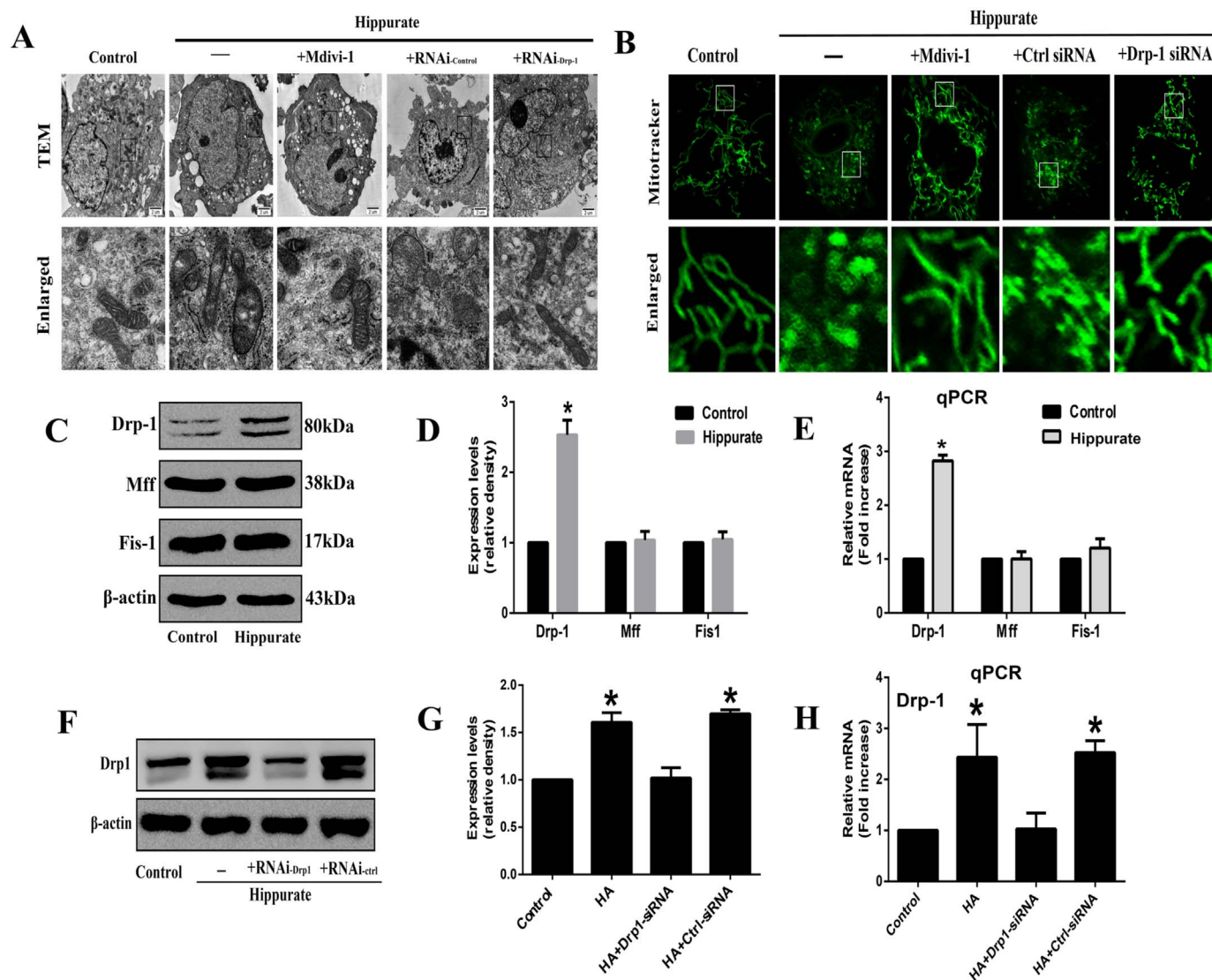


Fig. 2. Dynamin-related protein 1 (Drp1) mediates mitochondrial fission in hippurate-treated endothelial cells. Human aortic endothelial cells (HAECs) were treated with 4 mmol/l hippurate for 48 h. (A) Representative transmission electron microscopic (TEM) images of mitochondria in HAECs. (B) Mitochondria in HAECs were labeled with MitoTracker Green staining (original magnification 2400 ×), and mitochondrial morphology was analyzed using confocal laser-scanning microscopy. (C–E) Protein and mRNA levels of mitochondrial fission-related proteins (Drp1, Mff and Fis1) in HAECs exposed to hippurate. (F–H) HAECs were transfected with control siRNA (Ctrl-siRNA) or Drp1-siRNA for 6 h, then treated with 4 mmol/l hippurate for 48 h. Knockdown of Drp1 expression was assessed by western blot and qRT-PCR. * $P < 0.05$ vs. control.

mitochondrial membrane potential using the JC-1 dye. The results showed decreased mitochondrial membrane potential in the hippurate group, which was reversed by co-treatment with the Drp1 inhibitor (Fig. 3C, D).

3.5. Drp1 mediates hippurate-induced endothelial dysfunction

We further determined the physiological significance of Drp1 in hippurate-induced endothelial dysfunction in vitro. As shown in Fig. 3E–G, pretreatment with mdivi-1 and Drp1-specific siRNA transfection increased eNOS expression and attenuated ICAM-1 and vWF expression in HAECs. These data support the vital role of Drp1 in hippurate-induced endothelial dysfunction.

3.6. CKD and hippurate cause endothelial dysfunction in vivo

To validate the physiologic relevance of our in vitro data, we assessed endothelial function under conditions of CKD and hippurate treatment in vivo. Male Wistar rat assigned to the CKD group received 5/6 nephrectomy, and rats assigned to the hippurate group received

daily i.p. injections of 50 mg/kg hippurate. The general characteristics of the rats are shown in Table 1. Hippurate-treated rats displayed higher hippurate levels than control rats, with similar hippurate levels observed in ESRD patients, indicating that hippurate concentrations used for rat experiments are clinically relevant. 5/6 nephrectomy in the CKD group resulted in an almost sevenfold increase in plasma hippurate levels, which was consistent with the results of previous studies. Significantly higher serum creatinine levels were detected in the CKD group than in the sham group and no significant differences were observed between hippurate and control groups. Pathological observations of kidney tissue in different groups are shown in Supplemental Fig. 2.

We first identified whether CKD was associated with defective endothelial function. Compared with aortic rings from control rats, aortic rings from rats with CKD exhibited impaired Ach-mediated vasodilation (Fig. 5A) and reduced eNOS expression (Fig. 5E). In addition, endothelial dysfunction in CKD rats was reflected by elevated ICAM-1 and vWF levels (Fig. 5G, I, K). To determine whether the endothelial dysfunction in CKD rats is at least in part due to hippurate, we established a chronic hippurate model to increase plasma hippurate concentrations in

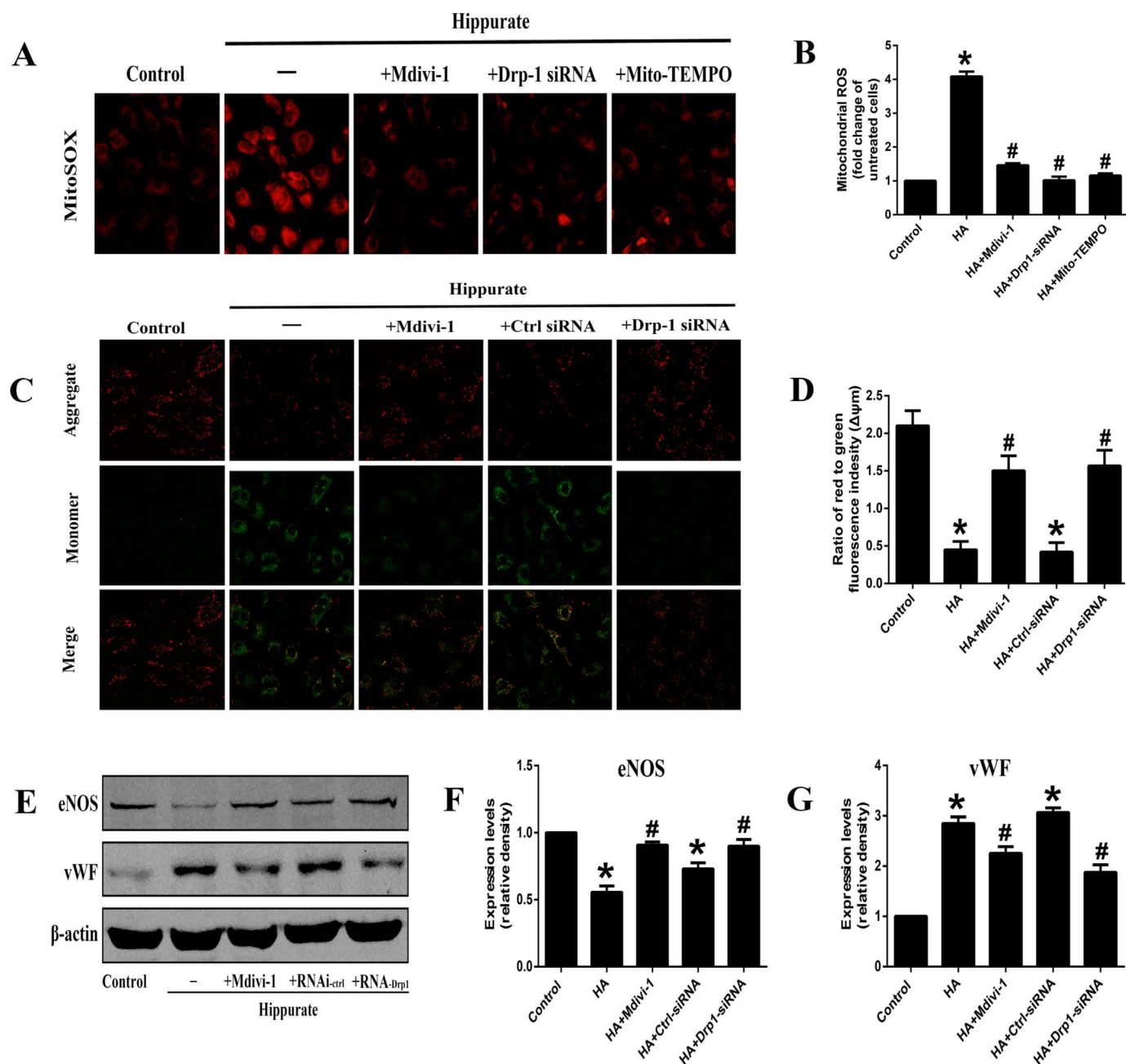


Fig. 3. Dynamin-related protein 1 (Drp1) mediates hippurate-induced endothelial dysfunction. (A, B) These cells were stained with MitoSOX Red to observe the change of mitochondrial ROS, and images were captured at × 200. (C, D) Changes in mitochondrial membrane potential (Δψm) by JC-1 staining (× 200). A decreased ratio of J-aggregates/monomer indicated a decreased mitochondrial membrane potential in hippurate group, whereas Drp1 inhibition could preserve mitochondrial membrane potential. (E–G) Expression of endothelial dysfunction-related proteins under the hippurate and Drp1 inhibition treatment. *P < 0.05 vs. control, #P < 0.05 vs. 4 mmol/l 48 h hippurate.

Table 1
General characteristics of hippurate-treated rats and CKD rats.

Parameter	Normal rats	Hippurate rats	Sham-operated rats	CKD rats
Serum creatinine (μmol/l)	32.0 ± 4.5	30.6 ± 13.4	29.2 ± 1.62	140.7 ± 27.5#
Triglycerides (mmol/l)	0.67 ± 0.25	1.11 ± 0.18*	0.58 ± 0.17	0.58 ± 0.17
Cholesterol (mmol/l)	1.65 ± 0.42	1.84 ± 0.15	1.76 ± 0.07	5.77 ± 1.27#
Serum hippurate (μmol/l)	6.35 ± 0.96	1972.2 ± 191.4*	6.21 ± 1.05	40.31 ± 1.98#

* P < 0.05 vs. normal rats.
P < 0.05 vs. sham-operated rats.

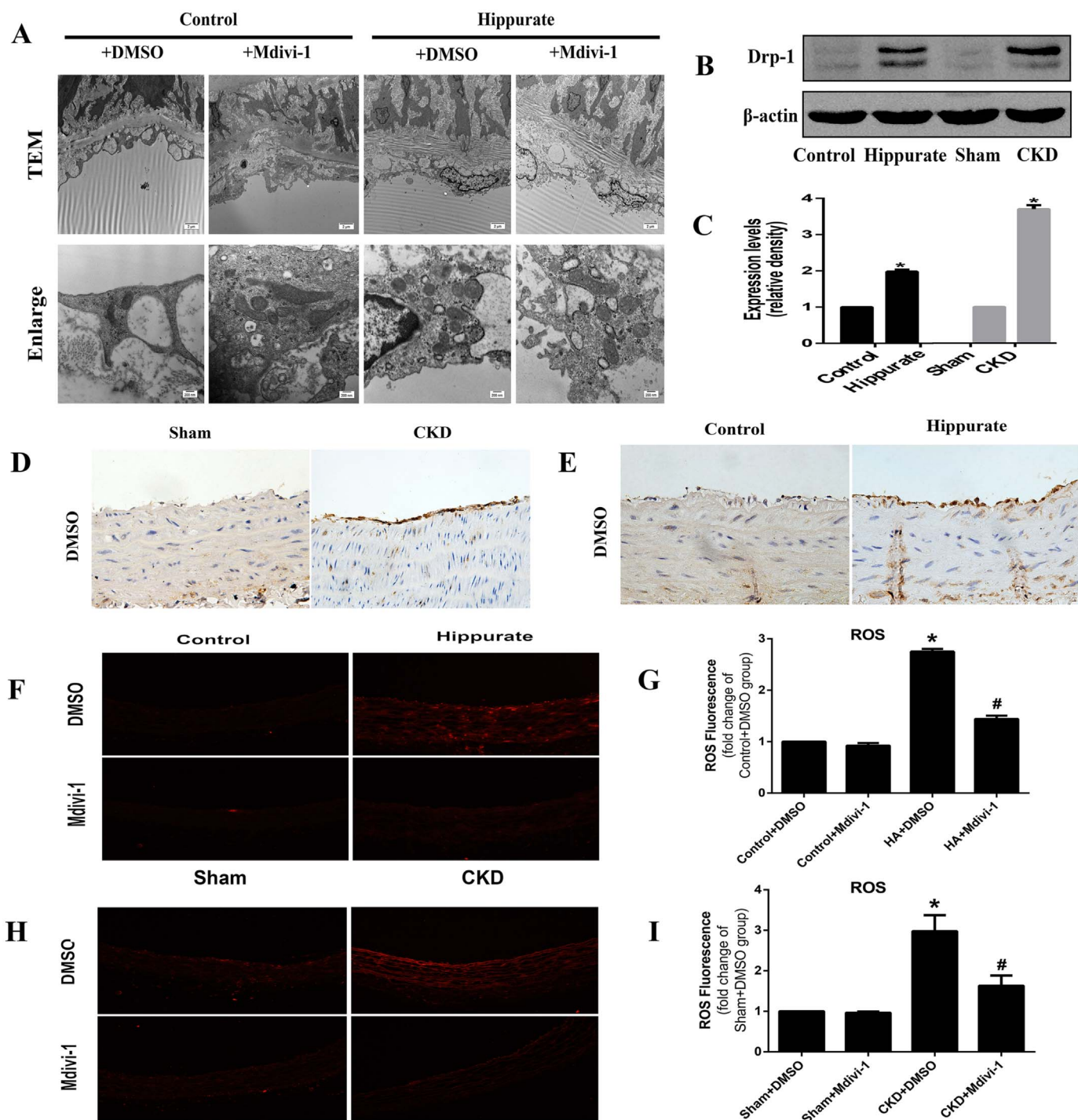


Fig. 4. Drp-1 mediated mitochondrial fission contributes to oxidative stress in aortas of CKD and hippurate-treated rat. (A) Representative transmission electron micrographs of mitochondria in the aortic endothelium of hippurate-treated rat. (original magnification $\times 4200$; scale bar = 2 μm ; enlarged magnification $\times 26500$; scale bar = 200 nm). (B–E) Expression of Drp1 in aortas of CKD and hippurate-treated rat analyzed by western blot and immunohistochemistry. (F–I) Intracellular ROS in aortas of CKD and hippurate-treated rat. Aortas were incubated with 5 mmol/l DHE in Krebs–Henseleit solution for 30 min and were observed under a fluorescence microscope ($\times 100$). * $P < 0.05$ vs. control/sham group.

healthy rats. Consistent with the CKD model, hippurate treatment significantly altered endothelial anti-inflammatory and antithrombotic properties in rats (Fig. 5C, F, H, J, L).

3.7. Upregulation of Drp1 expression and mitochondrial fragmentation in aortas of CKD and hippurate-treated rats

To determine whether mitochondrial fission is involved in endothelial dysfunction in vivo, we explored the expression of Drp1 in

endothelium via immunohistochemical staining and western blotting. Aortas from hippurate-treated and CKD rats exhibited higher levels of Drp1 than did aortas from control rats (Fig. 4B–E). We further assessed mitochondrial morphology in the aortic endothelium via electron microscopy. Compared with those in control rats, mitochondria in the aortic endothelium of hippurate-treated rats became swollen and spherical, and the number of mitochondria increased, indicative of enhanced mitochondrial fission. However, mdivi-1 reduced mitochondrial fragmentation, thereby preserving mitochondrial morphology

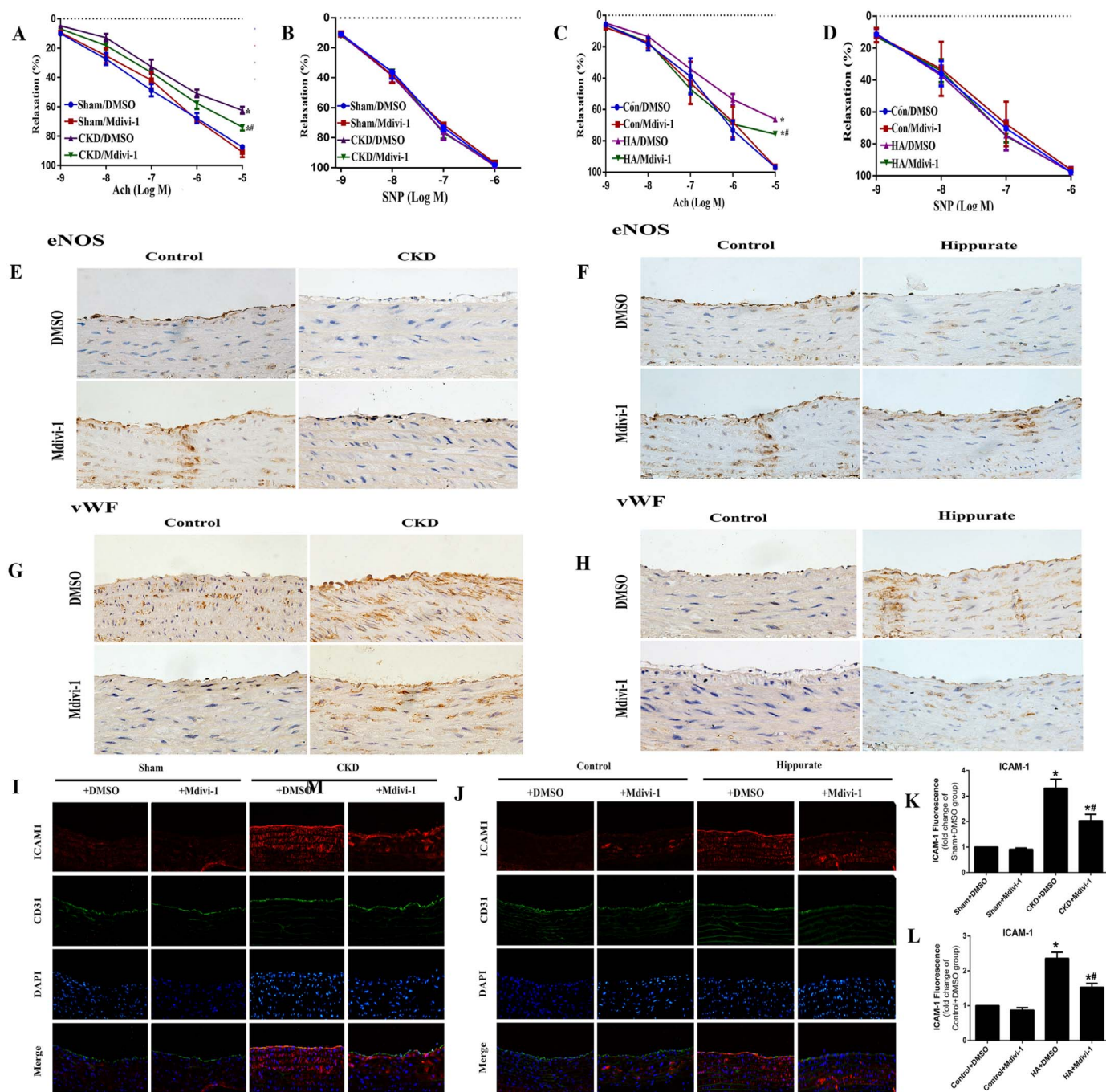


Fig. 5. Inhibition of mitochondrial fission attenuates endothelial dysfunction in CKD and hippurate-treated rat. (A, C) Endothelium-dependent vasodilator responses of CKD and hippurate-treated rat were measured in the presence of Acetylcholine (ACh) (10^{-9} – 10^{-5} mol/L). (B, D) Endothelium-independent vasodilator responses were measured in the presence of sodium nitroprusside (SNP) (10^{-9} – 10^{-6} mol/L). $n = 5$. Immunohistochemical staining for eNOS (E, F) and vWF (G, H) in aortas from CKD rat and hippurate-treated rat. Immunofluorescence staining for ICAM-1 (I–L) in aortas from CKD and hippurate-treated rat. * $P < 0.05$ vs. control/sham group, # $P < 0.05$ vs. hippurate/CKD group.

(Fig. 4A). In addition, the results of DHE staining showed an obvious increase in ROS production in hippurate-treated/CKD rat aortas, which was reversed by mdivi-1 (Fig. 3F–I).

3.8. Drp1 inhibition attenuates hippurate/CKD induced endothelial dysfunction in vivo

Finally, we sought to explore whether mdivi-1 treatment can attenuate endothelial dysfunction in hippurate-treated and CKD rats. Indeed, mdivi-1 treatment markedly improved endothelium-dependent vasodilation (Fig. 5A–D) and eNOS expression (Fig. 5E, F) and reduced vascular ICAM-1 and vWF expression (Fig. 5G–L). Immunoblot analysis

of endothelial dysfunction-related proteins under conditions of CKD and hippurate treatment in vivo also confirmed the results (Fig. 6A–D). These data suggested that Drp1 inhibition improved endothelial function in hippurate-treated/CKD rats.

4. Discussion

Patients with CKD are at high risk of CVDs and suffer from endothelial dysfunction. The relationship between uremic toxins and CVD and the potential mechanisms have been topics of great interest and active research. Previous studies have evidenced the endothelial toxicity of many important uremic toxins, such as uric acid, asymmetric

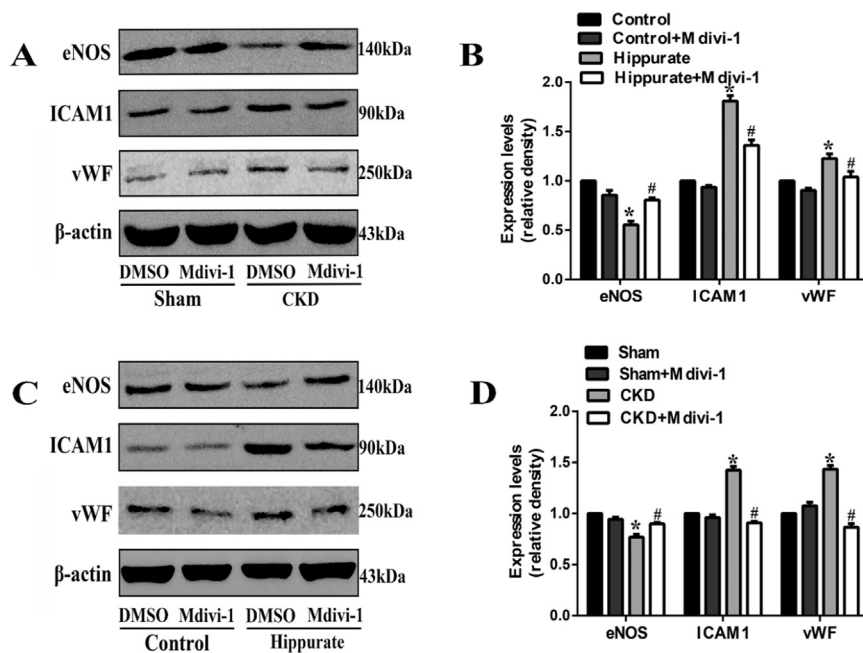


Fig. 6. Immunoblot analysis of endothelial dysfunction-related proteins under conditions of CKD and hippurate treatment in vivo. (A, B) Expression of endothelial dysfunction-related proteins (eNOS, ICAM-1, vWF) under conditions of CKD in vivo. (C, D) Expression of endothelial dysfunction-related proteins (eNOS, ICAM-1, vWF) under conditions of hippurate treatment in vivo. * $P < 0.05$ vs. control/sham group, # $P < 0.05$ vs. hippurate/CKD group.

dimethyl-arginine (ADMA), cyanate, indoxyl sulfate and p-cresyl sulfate. Hippurate, a major protein-bound toxin, can increase ROS production and may be associated with endothelial dysfunction and CVD [11,12]. However, there have been no studies that clearly explained the cardiovascular toxicity and detailed mechanism of hippurate. In this setting we tried to explore the role of hippurate in endothelial injury systematically. The results show that (1) hippurate promotes endothelial dysfunction by increasing mitoROS production; (2) Drp1 expression is upregulated in vitro and in vivo, and Drp1-mediated mitochondrial fission, at least in part, contributes to hippurate-induced endothelial dysfunction; and (3) the suppression of mitochondrial fission by Drp1 inhibition attenuates excessive mitoROS production and endothelial dysfunction. Our results suggest a causal link between hippurate and endothelial dysfunction for the first time. To the best of our knowledge, this is the first study to describe the role of Drp1 in mediating mitochondrial fission in uremia toxin-induced endothelial dysfunction.

CVD in patients with CKD, to a great extent, is attributed to endothelial dysfunction [4]. The following approaches can be employed to assess endothelial dysfunction: (1) functional tests, mainly endothelial-dependent vasodilation and (2) assessment of soluble biomarkers implicated in hemostasis, adherence, inflammation, and angiogenesis [22]. Nitric oxide (NO) is one of the most important vasorelaxant released by the endothelium. A reduction in eNOS levels is a marker of impaired endothelial function [23,24]. Cellular adhesion molecules, such as ICAM-1 and vascular cell adhesion molecule-1 (VCAM-1), are expressed on the surface of activated vascular endothelial cells. ICAM-1 and VCAM-1 mediate the migration and adhesion of leukocytes to the vascular endothelium and promote the inflammatory response to accelerate atherosclerosis. Previous studies have indicated that one important sign of endothelial dysfunction is the overexpression of ICAM-1/VCAM-1 [25,26]. In addition, upon endothelial dysfunction, cells release high levels of vWF, a glycoprotein involved in arterial thrombus formation, and this increase is also a marker of endothelial dysfunction [27–29]. In this study, using a rat model of CKD, we first confirmed that endothelial dysfunction can occur in CKD because of defects in endothelium-dependent vasodilation and eNOS expression. Although hippurate has been considered an important uremic toxin and reported to accelerate renal damage [30], its effect on the cardiovascular system, especially on the endothelium, has not been addressed. Here, we provide evidence that endothelial

dysfunction associated with CKD is at least in part mediated by hippurate. We established a concentration gradient of hippurate based on the concentration of hippurate in dialysis patients and confirmed that in endothelial cells, hippurate suppresses eNOS expression and upregulates ICAM-1 and vWF expression in a time- and concentration-dependent manner. In line with our in vitro results, chronic accumulation of hippurate in rats also promoted endothelial dysfunction, which was reflected by the impairment of endothelial-dependent vasodilation, reduction in eNOS expression and elevation in the levels of soluble biomarkers (ICAM1 and vWF). Previous studies have indicated that hippurate can augment oxidative stress by increasing ROS production [31]. ROS contributes significantly to endothelial dysfunction and even cardiovascular events [32]. Our study clearly shows that hippurate enhances mitoROS production, consistent with the results of previous studies. Meanwhile, the normalization of mitoROS production could ameliorate endothelial dysfunction. Collectively, these findings suggest that ROS derived from the mitochondria may be a key pathophysiological mechanism in hippurate-induced endothelial dysfunction.

The mitochondria play a key role in maintaining cellular functions and are dynamic organelles that undergo cycles of fusion and fission [33]. Accumulating evidence suggests that the disruption of mitochondrial dynamics and mitochondrial fragmentation is associated with mitochondrial oxidative damage and plays a causative role in the development of endothelial dysfunction. For example, endothelial damage and dysfunction under hypoxia/reoxygenation injury is thought to be due to increased mitochondrial fission [16,34]. In diabetes, high glucose levels disrupt normal mitochondrial dynamics leading to excessive mitochondrial fission, and these changes are subsequently responsible for excessive ROS production and endothelial dysfunction [15]. Mitochondrial fission is mainly modulated by Drp1, which triggers mitochondrial fission by binding with Fis1 or Mff on the mitochondria. In the current study, we observed altered mitochondrial morphology, reduced network, and increased Drp1 protein expression in endothelial cells exposed to hippurate and in hippurate-treated rats. Drp1 inhibition (via mdivi-1 or siDrp1) ameliorated hippurate-induced alterations in mitochondrial networks, ROS production and endothelial function, indicating the physiological significance of Drp1 and Drp1-mediated mitochondrial fission in hippurate-induced endothelial dysfunction.

Furthermore, we discuss the mechanisms of endothelial inflammatory response following release of mitochondrial ROS by

hippurate. ROS can mediate atherogenesis and endothelial inflammation by direct oxidative damage and by regulating redox-sensitive transcription factor NF- κ B. The accumulation of superoxide in endothelial cells can readily react with NO to form peroxynitrite, a compound that reduces NO bioavailability [35]. ROS can also promote tetrahydrobiopterin (BH4) oxidation, leading to the uncoupling of eNOS in the endothelium and decreased production of NO [36,37]. Besides, since eNOS-derived NO can prevent vascular inflammation [38], either a decrease in NO production or an increase in NO degradation can further lead to endothelial inflammatory response. In addition to the direct detrimental effects of ROS on endothelium, many studies have demonstrated that elevated ROS also mediate endothelial dysfunction by regulating NF- κ B. NF- κ B is a redox-sensitive transcription factor that regulates many genes. In unstimulated cells, NF- κ B exists in the cytoplasm as an inactive complex. Upon activation by ROS, active NF- κ B can translocate into the nucleus and bind to κ B consensus regulatory elements in the promoters of many responsive genes. Thus, NF- κ B can change the expression of certain genes [39]. In endothelial cells stimulated by cytokines (TNF- α) and uremic toxins (cyanate, uric acid), redox-sensitive NF- κ B suppresses eNOS mRNA and protein levels by decreasing mRNA stability [39–42]. Cytokines and toxins also activate the ICAM-1 and vWF genes through a cooperative interaction between NF- κ B and C/EBP binding to a composite enhancer element within the proximal promoter [43,44]. Based on the above studies, we find that most of these stimuli, in spite of their diversity, share similar signal pathway regulating endothelial inflammatory response via NF- κ B. Thus, we speculate that NF- κ B activation is also closely related to mitochondrial ROS and greatly contributes to hippurate-induced endothelial dysfunction in this setting. Further studies are required to confirm the role of NF- κ B in the interaction between hippurate and endothelial cells.

5. Conclusion

Our study supports a causal link between hippurate and endothelial dysfunction. Increased mitoROS via mitochondrial fission may be a contributing mechanism for endothelial dysfunction induced by hippurate.

Acknowledgements

This work was supported by the National Sciences Foundation of China [grant numbers 81471027, 81273968, 81072914 and 81401160]; Ministerial projects of the National Working Commission on Aging [grant number QLB2014W002]; and The Four hundred project of 301 [grant number YS201408]; Beijing Nova Program [grant number Z161100004916129].

Conflict of interest

The authors declare that they have no conflict of interest.

Appendix A. Supporting information

Supplementary data associated with this article can be found in the online version at <http://dx.doi.org/10.1016/j.redox.2018.03.010>.

References

- [1] E.L. Schiffrin, M.L. Lipman, J.F. Mann, Chronic kidney disease: effects on the cardiovascular system, *Circulation* 116 (2007) 85–97.
- [2] A.S. Go, et al., Chronic kidney disease and the risks of death, cardiovascular events, and hospitalization, *N. Engl. J. Med.* 351 (2004) 1296–1305.
- [3] U. Landmesser, H. Drexler, The clinical significance of endothelial dysfunction, *Curr. Opin. Cardiol.* 20 (2005) 547–551.
- [4] S.M. Hogas, et al., Methods and potential biomarkers for the evaluation of endothelial dysfunction in chronic kidney disease: a critical approach, *J. Am. Soc. Hypertens.* 4 (2010) 116–127.
- [5] M.J. Huang, et al., Blood coagulation system in patients with chronic kidney disease: a prospective observational study, *BMJ Open* 7 (2017) e014294.
- [6] C. Zoccali, Endothelial dysfunction and the kidney: emerging risk factors for renal insufficiency and cardiovascular outcomes in essential hypertension, *J. Am. Soc. Nephrol.* 17 (2006) S61–S63.
- [7] D. Rucker, M. Tonelli, Cardiovascular risk and management in chronic kidney disease, *Nat. Rev. Nephrol.* 5 (2009) 287–296.
- [8] S. Ito, M. Yoshida, Protein-bound uremic toxins: new culprits of cardiovascular events in chronic kidney disease patients, *Toxins* 6 (2014) 665–678.
- [9] F. Duranton, et al., Normal and pathologic concentrations of uremic toxins, *J. Am. Soc. Nephrol.* 23 (2012) 1258–1270.
- [10] R. Vanholder, et al., Review on uremic toxins: classification, concentration, and interindividual variability, *Kidney Int.* 63 (2003) 1934–1943.
- [11] F. Shang, et al., MicroRNA-92a mediates endothelial dysfunction in CKD, *J. Am. Soc. Nephrol.* (2017).
- [12] T. Shafi, et al., Results of the HEMO Study suggest that p-cresol sulfate and indoxyl sulfate are not associated with cardiovascular outcomes, *Kidney Int.* (2017).
- [13] T. Shafi, et al., Free levels of selected organic solutes and cardiovascular morbidity and mortality in hemodialysis patients: results from the Retained Organic Solutes and Clinical Outcomes (ROSCO) investigators, *PLoS One* 10 (2015) e0126048.
- [14] M. Ding, et al., Inhibition of dynamin-related protein 1 protects against myocardial ischemia-reperfusion injury in diabetic mice, *Cardiovasc. Diabetol.* 16 (2017) 19.
- [15] S.M. Shenouda, et al., Altered mitochondrial dynamics contributes to endothelial dysfunction in diabetes mellitus, *Circulation* 124 (2011) 444–453.
- [16] R.J. Giedt, et al., Mitochondrial fission in endothelial cells after simulated ischemia/reperfusion: role of nitric oxide and reactive oxygen species, *Free Radic. Biol. Med.* 52 (2012) 348–356.
- [17] D. Ormrod, T. Miller, Experimental uremia. Description of a model producing varying degrees of stable uremia, *Nephron* 26 (1980) 249–254.
- [18] X. Liu, et al., Altered KATP channel subunits expression and vascular reactivity in spontaneously hypertensive rats with age, *J. Cardiovasc. Pharmacol.* 68 (2016) 143–149.
- [19] S. Wang, et al., In vivo activation of AMP-activated protein kinase attenuates diabetes-enhanced degradation of GTP cyclohydrolase I, *Diabetes* 58 (2009) 1893–1901.
- [20] M. Hulsmans, E. Van Dooren, P. Holvoet, Mitochondrial reactive oxygen species and risk of atherosclerosis, *Curr. Atheroscler. Rep.* 14 (2012) 264–276.
- [21] T. Yu, J.L. Robotham, Y. Yoon, Increased production of reactive oxygen species in hyperglycemic conditions requires dynamic change of mitochondrial morphology, *Proc. Natl. Acad. Sci. USA* 103 (2006) 2653–2658.
- [22] N. Jourde-Chiche, et al., Vascular incompetence in dialysis patients—protein-bound uremic toxins and endothelial dysfunction, *Semin. Dial.* 24 (2011) 327–337.
- [23] M. Feletou, R. Kohler, P.M. Vanhoutte, Nitric oxide: orchestrator of endothelium-dependent responses, *Ann. Med.* 44 (2012) 694–716.
- [24] G. Yetik-Anacak, J.D. Catravas, Nitric oxide and the endothelium: history and impact on cardiovascular disease, *Vasc. Pharmacol.* 45 (2006) 268–276.
- [25] M.I. Cybulsky, M.A. Gimbrone Jr., Endothelial expression of a mononuclear leukocyte adhesion molecule during atherogenesis, *Science* 251 (1991) 788–791.
- [26] F.W. Lusinskas, et al., Cytokine-activated human endothelial monolayers support enhanced neutrophil transmigration via a mechanism involving both endothelial-leukocyte adhesion molecule-1 and intercellular adhesion molecule-1, *J. Immunol.* 146 (1991) 1617–1625.
- [27] G. Kirilov, et al., Increased plasma endothelin level as an endothelial marker of cardiovascular risk in patients with active acromegaly: a comparison with plasma homocysteine, *Methods Find. Exp. Clin. Pharmacol.* 31 (2009) 457–461.
- [28] U.M. Vischer, von Willebrand factor, endothelial dysfunction, and cardiovascular disease, *J. Thromb. Haemost.* 4 (2006) 1186–1193.
- [29] G.Y. Lip, A. Blann, von Willebrand factor: a marker of endothelial dysfunction in vascular disorders? *Cardiovasc. Res.* 34 (1997) 255–265.
- [30] M. Satoh, et al., Uremic toxins overload accelerates renal damage in a rat model of chronic renal failure, *Nephron Exp. Nephrol.* 95 (2003) e111–e118.
- [31] Y. Itoh, et al., Protein-bound uremic toxins in hemodialysis patients measured by liquid chromatography/tandem mass spectrometry and their effects on endothelial ROS production, *Anal. Bioanal. Chem.* 403 (2012) 1841–1850.
- [32] H. Li, S. Horke, U. Forstermann, Vascular oxidative stress, nitric oxide and atherosclerosis, *Atherosclerosis* 237 (2014) 208–219.
- [33] H. Otera, K. Mihara, Mitochondrial dynamics: functional link with apoptosis, *Int. J. Cell Biol.* 2012 (2012) 821676.
- [34] H. Zhou, et al., Mff-dependent mitochondrial fission contributes to the pathogenesis of cardiac microvasculature ischemia/reperfusion injury via induction of mROS-mediated cardiolipin oxidation and HK2/VDAC1 disassociation-involved mPTP opening, *J. Am. Heart Assoc.* 6 (2017).
- [35] M. Annuk, et al., Oxidative stress and endothelial function in chronic renal failure, *J. Am. Soc. Nephrol.* 12 (2001) 2747–2752.
- [36] H. Cai, D.G. Harrison, Endothelial dysfunction in cardiovascular diseases: the role of oxidant stress, *Circ. Res.* 87 (2000) 840–844.
- [37] S. Moncada, E.A. Higgs, Endogenous nitric oxide: physiology, pathology and clinical relevance, *Eur. J. Clin. Invest.* 21 (1991) 361–374.
- [38] V. Bauer, R. Sotnikova, Nitric oxide—the endothelium-derived relaxing factor and its role in endothelial functions, *Gen. Physiol. Biophys.* 29 (2010) 319–340.
- [39] C. Chen, et al., Soluble CD40 ligand induces endothelial dysfunction in human and porcine coronary artery endothelial cells, *Blood* 112 (2008) 3205–3216.
- [40] K.S. Lee, et al., Functional role of NF- κ B in expression of human endothelial nitric oxide synthase, *Biochem. Biophys. Res. Commun.* 448 (2014) 101–107.
- [41] W. Cai, et al., Uric acid induces endothelial dysfunction by activating the HMGB1/

- RAGE signaling pathway, *Biomed. Res. Int.* 2017 (2017) 4391920.
- [42] X. Wang, et al., Serum amyloid A induces endothelial dysfunction in porcine coronary arteries and human coronary artery endothelial cells, *Am. J. Physiol. Heart Circ. Physiol.* 295 (2008) H2399–H2408.
- [43] K.A. Roebuck, Oxidant stress regulation of IL-8 and ICAM-1 gene expression: differential activation and binding of the transcription factors AP-1 and NF-kappaB (Review), *Int. J. Mol. Med.* 4 (1999) 223–230.
- [44] Y. Liang, et al., Elevated levels of plasma TNF-alpha are associated with microvascular endothelial dysfunction in patients with sepsis through activating the NF-kappaB and p38 mitogen-activated protein kinase in endothelial cells, *Shock* 41 (2014) 275–281.